

1 Conference Proceedings Paper

2 **Investigating 2015-2019 deformation patterns at the**
3 **Methana volcano in Greece using Sentinel-1**
4 **MT-InSAR, GNSS/GPS and seismic data**

5 **Theodoros Gatsios** ^{1,2}, **Francesca Cigna** ^{3,*}, **Deodato Tapete** ³, **Vassilis Sakkas** ¹, **Kyriaki Pavlou** ¹
6 **and Issaak Parcharidis** ²

7 Published: date

8 Academic Editor: name

9 ¹ Department of Geophysics and Geothermy, National and Kapodistrian University of Athens (NKUA),
10 Panepistimiopolis-Zographou Athens 157 84, Greece; theogat@geol.uoa.gr (T.G.); vsakkas@geol.uoa.gr
11 (V.S.); kpavlou@geol.uoa.gr (K.P.)

12 ² Department of Geography, Harokopio University of Athens (HUA), 70 El. Venizelou Str., Athens 17671,
13 Greece; parchar@hua.gr

14 ³ Italian Space Agency (ASI), Via del Politecnico snc, Rome 00133, Italy; deodato.tapete@asi.it

15 * Correspondence: francesca.cigna@asi.it

16 **Abstract:** Methana is the westernmost dormant volcanic system belonging to the Hellenic volcanic
17 arc in Greece. Its last historic eruption occurred in ~230 BC, and no alarming signs were observed
18 in recent times. Nevertheless, seismic activity in the Saronic Gulf, geothermal manifestations, and
19 the proximity to densely populated regions (e.g. Athens), provide motivation for a dedicated
20 investigation into present-day deformation patterns. This study exploits Copernicus Sentinel-1 C-
21 band Synthetic Aperture Radar (SAR) images acquired in 2015–2019, processed with a Multi-
22 Temporal Interferometric SAR (MT-InSAR) approach using both persistent and distributed
23 scatterers. Geodetic data from permanent GNSS stations and 2006–2019 GPS benchmark surveying
24 are used as reference to calibrate the MT-InSAR results and validate their accuracy. Combination
25 with geological, seismological and geomorphological data, allows better understanding of the
26 observed ground deformation. The results suggest a complex displacement pattern across the
27 volcano, including local-scale processes, such as settlement in the suburban zones, mass movements
28 and some seasonal fluctuation overlapping with the long-term trend. This geoinformation can feed
29 into the volcano baseline hazard assessment and the monitoring system. Key findings are presented
30 in this short paper, while the full study is published in the journal *Applied Sciences*.

31 **Keywords:** SAR; InSAR; ground deformation; Sentinel-1; volcano monitoring; GNSS; seismicity;
32 ground deformation; slope instability; MT-InSAR
33

34 **1. Introduction**

35 The Methana peninsula in Greece is the westernmost dormant but geodynamically and
36 hydrothermally active [1], volcanic system belonging to the Hellenic volcanic arc. Its last historic
37 eruption occurred in ~230 BC, and no alarming signs were observed in recent times, so volcanic
38 hazard in Methana is considered “low” [2]. Nevertheless, seismic activity in the Saronic Gulf [3],
39 geothermal manifestations [1], and the proximity to densely populated regions (e.g. Athens), provide
40 motivation for a dedicated investigation into present-day deformation patterns.

41 In this context, the present study aims to investigate ground stability and motions at the Methana
42 volcano over the last five years, based on multi-temporal interferometric processing of Synthetic

43 Aperture Radar (SAR) satellite imagery, and integration of deformation estimates with an analysis of
44 regional seismicity and geodetic data from continuous Global Navigation Satellite System (GNSS)
45 monitoring and Global Positioning System (GPS) benchmark surveying.

46 Satellite Interferometric SAR (InSAR) has been largely exploited to study surface deformation at
47 many volcanic centers of the arc (e.g., [4–8]), proving its effectiveness to provide a spatially
48 distributed estimation of volcanic activity due to magma chamber processes, as well as shallow
49 deformation associated to hydrothermal activity. Despite this abundant literature, to the best of our
50 knowledge, no InSAR investigation has been previously focused on Methana, therefore the present
51 study aims to start filling this knowledge gap.

52 Key findings from this integrated analysis are presented in this paper. For the detailed analysis
53 and discussion of the results, the reader can refer to the full article published in the journal *Applied*
54 *Sciences* [9].

55 2. Experiments

56 2.1. Seismic Data Analysis

57 The database of the seismological laboratory of the National and Kapodistrian University of
58 Athens (NKUA; http://dggsl.geol.uoa.gr/en_index.html) was exploited for the analysis of regional
59 seismicity in the 2006–2019 period.

60 The optimization of epicentres was carried out using the HYPOINVERSE software [10], and the
61 data were divided into two time intervals: (i) January 2006 to August 2019, i.e. the time period covered
62 by the GNSS data; and (ii) March 2015 to August 2019, i.e. the MT-InSAR time span.

63 2.2. GNSS and GPS Monitoring

64 Two benchmark stations were established in 2006 in the northern (i.e. station MENO) and
65 southern (MESO) sector of Methana [11], as part of a larger GPS network aiming to study ground
66 deformation in the north-western part of the Hellenic volcanic arc. The stations were re-occupied
67 several times up to December 2019 using Leica receivers (SR9500 and AX1200).

68 Since August 2019, cGNSS data were available from the MTNA station located in the western
69 part of the peninsula, and part of the GNSS network of the Institute of Geodynamics, National
70 Observatory of Athens (NOA). Horizontal velocity records from two more cGNSS stations were also
71 available from the National Technical University of Athens (NTUA), i.e. station METH installed in
72 2004 in the southern sector of Methana, and from [12], i.e. station 010A located to the south-east of
73 the peninsula, at Poros. Moreover, a continuous GNSS (cGNSS) station was established in early 2015
74 at Lygourio (LYGO), as part of the HxGN SmartNet (<https://gr.nrtk.eu/>), and since then it acts as local
75 reference station. For this reason, the regional velocity vector estimated at LYGO was subtracted from
76 the two local GPS benchmark stations, as well as the two other sites (i.e. METH and 010A), with the
77 aim to better define the local deformation field of the peninsula.

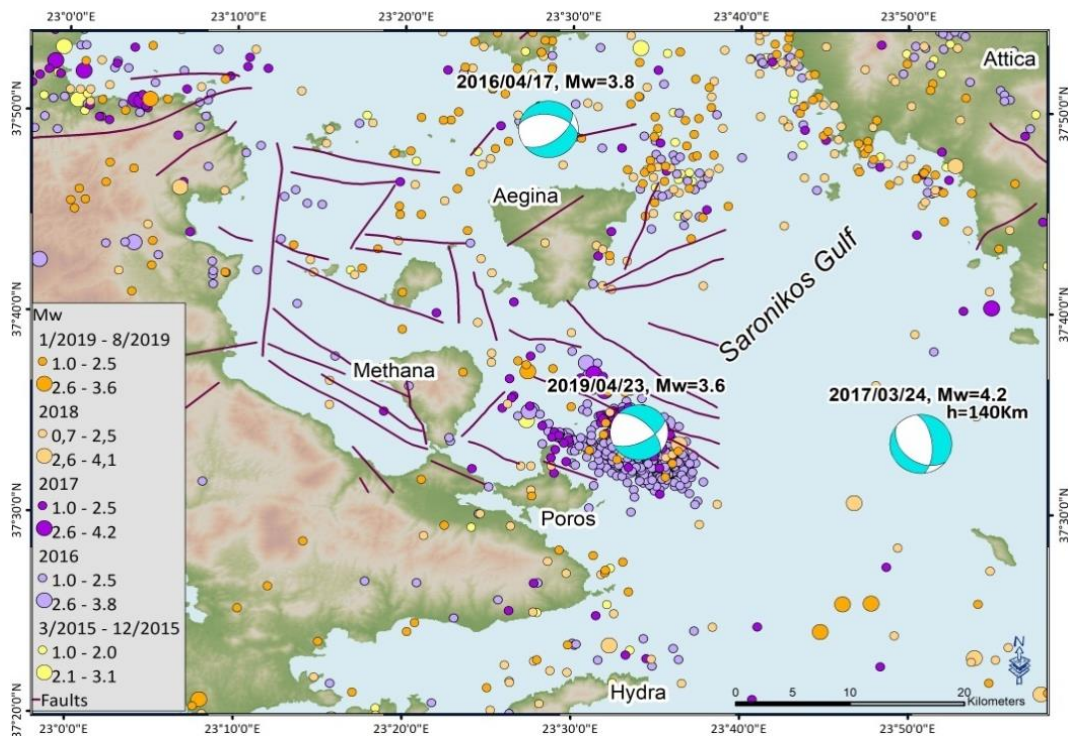
78 2.3. Satellite MT-InSAR Investigation

79 A long data stack of 99 SAR images acquired by the Copernicus Sentinel-1 constellation in
80 ascending mode in the period March 2015 – August 2019 was exploited. These data are in
81 Interferometric Wide (IW) swath mode [13], and provide a 250 km large coverage, with pixel
82 resolutions of 5 m and 20 m (single look) in range and azimuth, respectively.

83 The stack was processed using an advanced Multi-Temporal InSAR (MT-InSAR) approach, an
84 extension of the basic technique of Differential InSAR (DInSAR; e.g. [14]). The method used both
85 Persistent Scatterers (PS) and Distributed Scatterers (DS), in order to enhance the coverage of
86 monitoring targets in sub-urban and rural areas. The GAMMA SAR and Interferometry software and
87 the Interferometric Point Target Analysis (IPTA) method [15] were used for the multi-temporal
88 analysis.

89 **3. Results and Discussion**

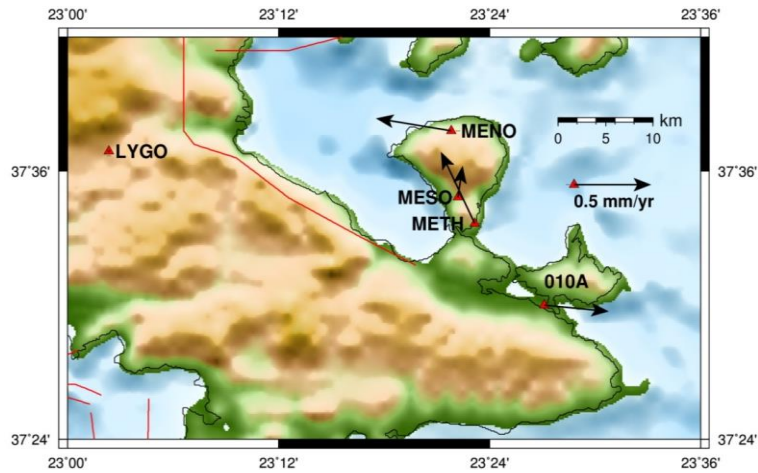
90 The seismic data analysis shows that the Saronikos Gulf region is mainly characterized by
 91 moderate seismic events and shallow depths, as already discussed in the literature [16]. In 2015–2019
 92 (Figure 1), three significant seismic events occurred in the area: two moderate shallow earthquakes
 93 with magnitudes $M_w=3.8$, and $M_w=3.6$, and a very deep one (depth=142 km) with magnitude
 94 $M_w=4.2$. A significant seismic swarm was observed NE of Poros Island. The seismic activity in this
 95 cluster started in 2016 and continued with few events up to 2019. Additional to the surface seismicity,
 96 very deep (80–100 km) sporadic micro events took place on a wider area extending from Methana
 97 towards Hydra Island. These deep micro-events may be attributed to the NE-subduction zone of the
 98 Ionian oceanic plate that reaches very deep in this area [3,11,17,18].



99
100 **Figure 1.** Seismic activity recorded in March 2015–August 2019. Full paper source: [9].

101 Geodetic monitoring results at the two local benchmark stations MENO and MESO for the
 102 period 2006–2019 appeared consistent with the regional velocity field. Although the resulting
 103 horizontal velocity vectors are very small (< 1 mm/year) and indicate a uniform deformation of the
 104 broader Methana area, a pattern of differential motion can be distinguished (Figure 2). The northern
 105 station (i.e. MENO) exhibited westward motion, while the southern sites (i.e. MESO and METH)
 106 showed northward motion (though velocity values are small, and errors significant). The more
 107 evident differential behaviour is found in the vertical component at the MESO station, which
 108 exhibited noticeable subsidence, to correlate with MT-InSAR findings.

109 The MT-InSAR processing extracted 4769 PS targets and 6234 DS targets (Figure 3), mostly
 110 located at low altitudes (up to ~ 100 – 150 m a.s.l. for the PS, and up to ~ 350 – 400 m a.s.l. for the DS),
 111 where there are urban settlements, and also on geological formations which exhibit high coherence,
 112 such as volcanoclasts. The uncertainty observed in the estimated Line-Of-Sight (LOS) velocity V_{Los} is
 113 2.8 mm/year on average for the PS dataset, and 2.6 mm/year for the DS dataset. These values provide
 114 an indication of the precision of the MT-InSAR results, and also suggest that the ± 3.0 mm/year V_{Los}
 115 interval can be considered as the velocity range indicating stability (green points in Figure 3).

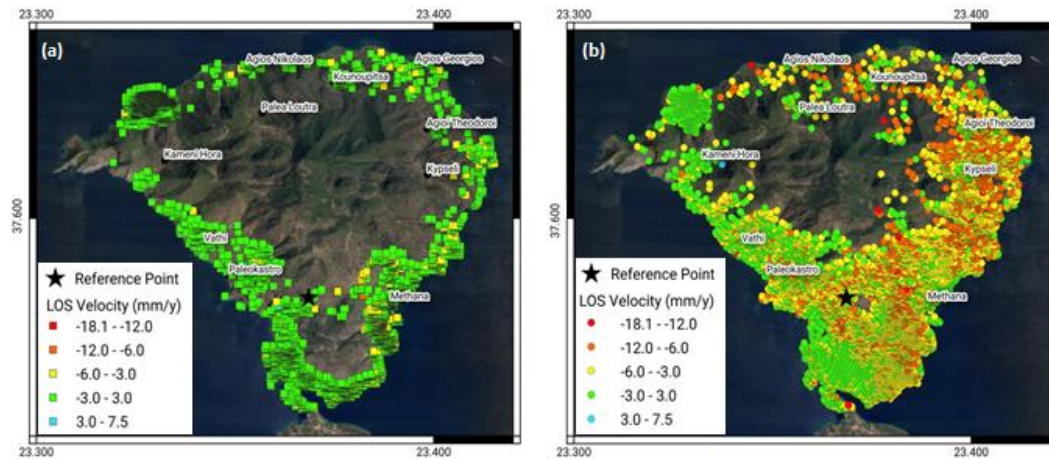


116

117

118

Figure 2. Local horizontal velocity field 2006–2019 calculated with respect to the LYGO cGNSS site in the broader area of Methana peninsula. Full paper source: [9].



119

120

121

122

123

Figure 3. Line-of-sight (LOS) deformation velocity in 2015–2019 from the Multi-Temporal Interferometric Synthetic Aperture Radar (MT-InSAR) analysis for the (a) Persistent Scatterers (PS) and (b) Distributed Scatterers (DS) datasets, overlapped onto satellite optical imagery (© 2020 TerraMetrics, © 2020 Google). Full paper source: [9].

124

125

126

127

128

129

130

131

132

133

134

135

136

137

138

139

140

The accuracy of the MT-InSAR results was also estimated at the GPS benchmark stations MESO and MENO, after conversion of their local velocity values to the LOS direction using a frame of reference transformation (full details available in the full paper [9]).

After calibration, the maximum V_{LOS} observed was -18.1 mm/year away from the sensor (i.e. negative values). PS and DS moving faster are located on the eastern flank of the peninsula and, considering the LOS geometry, these could plausibly indicate occurrence of downslope mass movements and slope instability in rugged terrain and volcanic landforms that are recognized as prone to landsliding and rock-falls [19]. These concentrate on the volcanic ranges and gully erosion landforms above the urban settlements of Methana, Kipseli, Agii Teodori and Agios Georgios.

The northern portion of Methana town is built onto alluvium, and it seems slightly more stable ($V_{LOS} = -1.8$ mm/year) than the central zone of the town (built onto volcanoclastics), which is moving away from the satellite at -2.5 mm/year. Overall, it appears that the majority of the urban area footprint is not affected by significant deformation, while somehow greater rates are found in the sub-urban zones, as revealed by the DS targets.

No significant deformation pattern is found across the sparsely-vegetated outcrops at Mavri Petra. However, evidence of seasonal deformation can be detected in the time-series, with amplitude of approximately 5 mm, and periodicity of 1 year.

141 **4. Conclusions**

142 2015–2019 observations from the MT-InSAR and GNSS/GPS analysis are compatible with the
 143 anticipated “low” volcanic activity of Methana. The overall spatial distribution of the PS deformation
 144 values does not shape into a deformation field that could be reliably attributed to a typical volcanic
 145 inflation/deflation dynamic of the whole Methana, as found in the literature for other active volcanic
 146 areas. On the other side, the DS dataset may suggest the presence of deformation patterns along the
 147 eastern flank, though only in some cases these associate with specific landforms (e.g. narrow valleys,
 148 erosion gullies, superficial slides). No strong seismic events ($M_w > 4$) or intense seismicity was
 149 recorded in the peninsula. Moreover, neither the location, the depth nor the magnitude of seismic
 150 events occurred in the vicinity could be directly associated with the observed ground deformation.

151 The interpreted low level of activity is clearly the initial baseline above which further
 152 investigations need to be conducted to improve our understanding of the long-term deformation
 153 behavior of the peninsula and the potential risk for the densely populated areas in its proximity.

154 **Acknowledgments:** Copernicus Sentinel-1 data were accessed through the Sentinel Hub platform and processed
 155 using the GAMMA SAR and Interferometry software licensed to Harokopio University of Athens, and ESA’s
 156 SNAP software. GNSS data were provided by NTUA for METH station, by HxGN SmartNet for LYGO station,
 157 and by the Institute of Geodynamics of NOA for MTNA and 010A stations. Seismic data were provided by the
 158 Department of Geophysics and Geothermy, NKUA. High-resolution DSM was provided by the Hellenic
 159 Mapping and Cadastral Organisation. Some of the figures were created with the GMT software [20].

160 **Funding:** Remeasurement of the GPS benchmarks MESO and MENO was financed by “HELPOS—Hellenic Plate
 161 Observing System” (MIS 5002697), which is implemented under the action “Reinforcement of the Research and
 162 Innovation Infrastructure”, funded by the Operational Programme “Competitiveness, Entrepreneurship and
 163 Innovation” (NSRF 2014-2020) and co-financed by Greece and the EU (European Regional Development Fund).

164 **Author Contributions:** conceptualization, F.C., D.T. and I.P.; methodology, T.G., F.C., D.T. and V.S.; software,
 165 T.G., V.S. and K.P.; validation, T.G., V.S. and K.P.; formal analysis, T.G., F.C., D.T., V.S. and K.P.; investigation,
 166 T.G., F.C., D.T., V.S. and K.P.; resources, I.P.; data curation, T.G., V.S. and K.P.; writing—original draft
 167 preparation, T.G., F.C., D.T., V.S. and K.P.; writing—review and editing, I.P.; supervision, F.C. and I.P. All
 168 authors have read and agreed to the published version of the manuscript.

169 **Conflicts of Interest:** The authors declare no conflict of interest.

170 **References**

- 171 1. D’Alessandro, W.; Brusca, L.; Kyriakopoulos, K.; Michas, G.; Papadakis, G. Methana, the westernmost
 172 active volcanic system of the south Aegean arc (Greece): Insight from fluids geochemistry. *J. Volcanol.*
 173 *Geotherm. Res.* **2008**, *178*, 818–828, doi:10.1016/j.jvolgeores.2008.09.014.
- 174 2. Vougioukalakis, G.E.; Fytikas, M. Volcanic hazards in the Aegean area, relative risk evaluation, monitoring
 175 and present state of the active volcanic centers. *Dev. Volcanol.* **2005**, *7*, 161–183, doi:10.1016/S1871-
 176 644X(05)80037-3.
- 177 3. Makris, J.; Papoulia, J.; Drakatos, G. Tectonic deformation and microseismicity of the Saronikos Gulf,
 178 Greece. *Bull. Seismol. Soc. Am.* **2004**, *94*, 920–929, doi:10.1785/0120020209.
- 179 4. Parcharidis, I.; Lagios, E. Deformation in Nisyros volcano (Greece) using differential radar interferometry.
 180 *Bull. Geol. Soc. Greece* **2001**, *34*, 1587, doi:10.12681/bgsg.17267.
- 181 5. Sachpazi, M.; Kontoes, C.; Voulgaris, N.; Laigle, M.; Vougioukalakis, G.; Sikioti, O.; Stavrakakis, G.;
 182 Baskoutas, J.; Kalogeras, J.; Lepine, J.C. Seismological and SAR signature of unrest at Nisyros caldera,
 183 Greece. *J. Volcanol. Geotherm. Res.* **2002**, *116*, 19–33, doi:10.1016/S0377-0273(01)00334-1.
- 184 6. Lagios, E.; Sakkas, V.; Parcharidis, I.; Dietrich, V. Ground deformation of Nisyros Volcano (Greece) for the
 185 period 1995-2002: Results from DInSAR and DGPS observations. *Bull. Volcanol.* **2005**, *68*, 201–214,
 186 doi:10.1007/s00445-005-0004-y.
- 187 7. Foumelis, M.; Trasatti, E.; Papageorgiou, E.; Stramondo, S.; Parcharidis, I. Monitoring Santorini volcano
 188 (Greece) breathing from space. *Geophys. J. Int.* **2013**, *193*, 161–170, doi:10.1093/gji/ggs135.
- 189 8. Papageorgiou, E.; Foumelis, M.; Trasatti, E.; Ventura, G.; Raucoules, D.; Mouratidis, A. Multi-sensor SAR
 190 geodetic imaging and modelling of santorini volcano post-unrest response. *Remote Sens.* **2019**, *11*,

- 191 doi:10.3390/rs11030259.
- 192 9. Gatsios, T.; Cigna, F.; Tapete, D.; Sakkas, V.; Pavlou, K.; Parcharidis, I. Copernicus Sentinel-1 MT-InSAR,
193 GNSS and Seismic Monitoring of Deformation Patterns and Trends at the Methana Volcano, Greece. *Appl.*
194 *Sci.* **2020**, *10*, 6445, doi:10.3390/app10186445.
- 195 10. Klein, F.W. *User's guide to HYPOINVERSE, a program for VAX computers to solve for earthquake locations and*
196 *magnitudes*; 1989;
- 197 11. Papageorgiou, E. Crustal movements along the NW Hellenic volcanic arc from DGPS measurements. *Bull.*
198 *Geol. Soc. Greece* **2010**, *43*, 331, doi:10.12681/bgs.11185.
- 199 12. Chousianitis, K.; Ganas, A.; Gianniou, M. Kinematic interpretation of present-day crustal deformation in
200 central Greece from continuous GPS measurements. *J. Geodyn.* **2013**, *71*, 1–13, doi:10.1016/j.jog.2013.06.004.
- 201 13. Torres, R.; Snoeij, P.; Geudtner, D.; Bibby, D.; Davidson, M.; Attema, E.; Potin, P.; Rommen, B.Ö.; Flourey,
202 N.; Brown, M.; et al. GMES Sentinel-1 mission. *Remote Sens. Environ.* **2012**, *120*, 9–24,
203 doi:10.1016/j.rse.2011.05.028.
- 204 14. Bamler, R.; Hartl, P. Synthetic aperture radar interferometry. *Inverse Probl.* **1998**, *14*, R1, doi:10.1088/0266-
205 5611/14/4/001.
- 206 15. Werner, C.; Wegmüller, U.; Strozzi, T.; Wiesmann, A. Interferometric Point Target Analysis for
207 Deformation Mapping. In Proceedings of the International Geoscience and Remote Sensing Symposium
208 (IGARSS); 2003; Vol. 7, pp. 4362–4364.
- 209 16. Makropoulos, K.; Kaviris, G.; Kouskouna, V. An updated and extended earthquake catalogue for Greece
210 and adjacent areas since 1900. *Nat. Hazards Earth Syst. Sci.* **2012**, *12*, 1425–1430, doi:10.5194/nhess-12-1425-
211 2012.
- 212 17. Karakonstantis, A.; Papadimitriou, P.; Millas, C.; Spingos, I.; Fountoulakis, I.; Kaviris, G. Tomographic
213 imaging of the NW edge of the Hellenic volcanic arc. *J. Seismol.* **2019**, *23*, 995–1016, doi:10.1007/s10950-019-
214 09849-8.
- 215 18. Papanikolaou, D.; Lykousis, V.; Chronis, G.; Pavlakis, P. A comparative study of neotectonic basins across
216 the Hellenic arc: the Messiniakos, Argolikos, Saronikos and Southern Evoikos Gulfs. *Basin Res.* **1988**, *1*, 167–
217 176, doi:10.1111/j.1365-2117.1988.tb00013.x.
- 218 19. Antoniou, V.; Nomikou, P.; Bardouli, P.; Lampridou, D.; Ioannou, T.; Kalisperakis, I.; Stentoumis, C.;
219 Whitworth, M.; Krokos, M.; Ragia, L. An Interactive Story Map for the Methana Volcanic Peninsula. In
220 Proceedings of the Proceedings of the 4th International Conference on Geographical Information Systems
221 Theory, Applications and Management (GISTAM 2018); Scitepress, 2018; pp. 68–78.
- 222 20. Wessel, P.; Smith, W.H.F. New, improved version of Generic Mapping Tools released. *EOS Trans AGU*
223 **1998**, *79*, 579, doi:10.1029/98EO00426.
- 224



© 2020 by the authors; licensee MDPI, Basel, Switzerland. This article is an open access article distributed under the terms and conditions of the Creative Commons by Attribution (CC-BY) license (<http://creativecommons.org/licenses/by/4.0/>).